V3. Submitted to ApJL

Estimating Be Star Disk Radii using Hα Emission Equivalent Widths

Erika D. Grundstrom and Douglas R. Gies

Center for High Angular Resolution Astronomy and
Department of Physics and Astronomy,
Georgia State University, P. O. Box 4106, Atlanta, GA 30302-4106;
erika@chara.gsu.edu, gies@chara.gsu.edu

ABSTRACT

We present numerical models of the circumstellar disks of Be stars, and we describe the resulting synthetic Hα emission lines and maps of the wavelength-integrated emission flux projected onto the sky. We demonstrate that there are monotonic relationships between the emission line equivalent width and the ratio of the angular half-width at half maximum of the projected disk major axis to the radius of the star. These relationships depend mainly upon the temperatures of the disk and star, the inclination of the disk normal to the line of sight, and the adopted outer boundary for the disk radius. We show that the predicted Hα disk radii are consistent with those observed directly through long baseline interferometry of nearby Be stars (especially once allowance is made for disk truncation in binaries and for dilution of the observed Hα equivalent width by continuum disk flux in the V-band).

Subject headings: stars: emission-line, Be — circumstellar matter — techniques: interferometric — techniques: spectroscopic

1. Hα Spectral and Spatial Emission Models

Be stars are rapidly rotating B-type stars that lose mass into an equatorial, circumstellar disk (Porter & Rivinius 2003). The disk flux is observed in emission lines (especially the hydrogen Hα line), an infrared excess, and the polarization of starlight scattered in the disk. It is now possible to investigate the actual extent and geometry of the circumstellar disks through optical long baseline interferometry of nearby Be stars (Stee et al. 1995; Quirrenbach

et al. 1997; Chesneau et al. 2005; Tycner et al. 2005, 2006). Most of these investigations have focused on the angular resolution of the disks in a narrow spectral band centered on the Hα emission line. The long baseline interferometric observations are limited to the nearby sample of Be stars at present, so we need other indirect methods to help estimate the sizes of Be star disks in more distant targets.

Here we explore how the disk radius may be estimated from measurements of the disk Hα emission flux. We begin with an idealized case to illustrate some of the important parameters that define the relationship between equivalent width and radius. Suppose that the disk is isothermal and geometrically thin and that the line emission is dominated by an inner optically thick region that appears as an ellipse projected onto the plane of the sky. We also make the simplifying assumption that the specific intensity of the disk emission I_λ^d is isotropic. Then the wavelength integrated Hα flux will depend on the product of the surface flux, the wavelength range where Hα is optically thick, and the projected solid angle,

$$F(\mathrm{H}\alpha) = \pi I_\lambda^d < \triangle\lambda > \cos i \left(\frac{R_d}{D}\right)^2 \tag{1}$$

where $< \triangle\lambda >$ is the wavelength interval over which the line is optically thick (averaged over the visible disk), i is the disk normal inclination angle, R_d is the boundary radius of the optically thick disk, and D is the distance to the star. We measure this flux through the emission equivalent width W_λ, which is given in wavelength units relative to the local continuum flux,

$$F(\mathrm{H}\alpha) = |W_\lambda|(1+\epsilon)\pi I_\lambda^s \left(\frac{R_s}{D}\right)^2 \tag{2}$$

where ϵ is the ratio of disk continuum flux to stellar flux in the Hα region, I_λ^s is the stellar specific intensity near Hα (assumed isotropic), and R_s is the radius of the star. We can then equate these two expressions to find the predicted relationship between the ratio of disk to stellar radius and Hα emission equivalent width,

$$\frac{R_d}{R_s} = \sqrt{\frac{I_\lambda^s}{I_\lambda^d}\frac{W_\lambda(1+\epsilon)}{< \triangle\lambda > \cos i}}. \tag{3}$$

This special case is characterized by a disk radius that varies as the square root of the emission equivalent width, and this expectation is supported by the interferometric observations of Tycner et al. (2005) who find that the emitted Hα flux scales with the square of the disk radius. However, the coefficient of the relationship also depends on the ratio of the stellar to disk specific intensities that is dependent upon the stellar and disk temperatures. Furthermore, there is an inclination dependence in both the $\cos i$ projection factor and the

$< \triangle\lambda >$ term (through the range in velocities and Doppler shifts viewed through the disk). The $< \triangle\lambda >$ term also depends upon the assumed disk density since the optical depth is based on the product of neutral hydrogen density and the emission line profile. Finally, there must also be some emission contribution from the optically thin outer disk that is ignored in expression above. Thus, in order to predict accurately the relationship between equivalent width and disk radius, we need a more complete model that accounts for the specific dependences on disk temperature, inclination, and density.

We have adopted the Be disk model approach of Hummel & Vrancken (2000) that is based upon models developed by Horne & Marsh (1986) and Horne (1995) for accretion disks in cataclysmic variables. The disk is assumed to be axisymmetric and centered over the equator of the underlying star, and the gas density varies as

$$\rho(R, Z) = \rho_0 R^{-n} \exp\left[-\frac{1}{2}\left(\frac{Z}{H(R)}\right)^2\right] \tag{4}$$

where R and Z are the radial and vertical cylindrical coordinates (in units of stellar radii), ρ_0 is the base density at the stellar equator, n is a radial density exponent, and $H(R)$ is the disk vertical scale height. The neutral hydrogen population within the disk is found by equating the photoionization and recombination rates (Gies et al. 2006). The disk gas is assumed to be isothermal and related to the stellar effective temperature $T_{\rm eff}$ by $T_d = 0.6T_{\rm eff}$ (Carciofi & Bjorkman 2006).

The numerical model represents the disk by a large grid of azimuthal and radial surface elements, and the equation of transfer is solved along a ray through the center of each element according to

$$I_\lambda = S_\lambda^L(1 - e^{-\tau_\lambda}) + I_\lambda^s e^{-\tau_\lambda} \tag{5}$$

where I_λ is the derived specific intensity, S_λ^L is the source function for the disk gas (taken as the Planck function for the disk temperature T_d), I_λ^s is the specific intensity for a uniform disk star (taken as the product of the Planck function for $T_{\rm eff}$ and an Hα photospheric absorption line derived from the grid of Martins et al. 2005), and τ_λ is the integrated optical depth along the ray (for assumed Keplerian rotation; see eq. [4] in Horne 1995 and eq. [7] in Hummel & Vrancken 2000). The first term applies to all the disk area elements that are unocculted by the star (see eq. [12] in Hummel & Vrancken 2000) while the second term applies to all elements that correspond to the projected photospheric disk of the star. The absorption line adopted in I_λ^s is Doppler shifted according to solid body rotation for the photospheric position in a star that is rotating at 90% of the critical value.

The model code calculates a synthetic line profile over the range from -2000 to $+2000$ km s^{-1} at 10 km s^{-1} intervals by summing the product of projected area and specific intensity

over the disk grid. We then integrate the line profile relative to the continuum to form a predicted equivalent width (taken as positive for net absorption or negative for net emission). The model also forms a synthetic image of the star plus disk in the plane of the sky by summing the intensity over a 2.8 nm band centered on Hα. We collapsed this image along the projected major axis to get the summed spatial intensity, and then we determined the radius where the summed intensity drops to half its maximum value (excluding the spatial range corresponding to photospheric intensity). We adopt this half-maximum summed intensity radius as the effective disk radius in the following discussion.

We need to specify the stellar mass and radius in the code in order to determine the disk Keplerian velocities, and we adopted these as a function of stellar effective temperature (or spectral subtype) using the eclipsing binary results for B-stars from Harmanec (1988). We determined the relationship between model equivalent width and disk radius by running a sequence of models defined by the spectral subtype of the star, the disk inclination, the disk radial density exponent n, and the selected value for the outer boundary of the disk. The final variable for any sequence is the base density ρ_0, and we computed models over a range in ρ_0 that corresponds to Hα profiles with no visible emission up to strong emission cases with $|W_\lambda| > 50$ Å.

We show the predicted relationship between the disk radius and Hα equivalent width in Figure 1 for the case of a B2 Ve star ($T_{\rm eff} = 23100$ K) assuming $n = 3.0$ and an outer boundary at $100R_s$. The lower solid line shows the pole-on case ($i = 0°$). At higher inclination angles ($i = 50°$ and $i = 80°$ for the middle and top lines, respectively) the projected disk area is smaller ($\propto \cos i$), and consequently the emission equivalent width is smaller for a given disk radius. We do not show the $i = 90°$ case because the shear broadening approximation for the emission profile width breaks down for an edge-on orientation (Horne & Marsh 1986). The symbols along each sequence indicate positions of fiducial base density values. Note that all three curves show the expected square root dependence predicted for the simple case (eq. [3] above).

The three dashed lines in Figure 1 show the corresponding inclination cases for a B8 Ve star ($T_{\rm eff} = 11600$ K) again made assuming $n = 3.0$ and an outer boundary at $100R_s$. These curves are all shifted to the left relative to the B2 Ve sequences because the photospheric absorption component is larger in cooler B-stars. The model profiles of the B8 Ve sequence have less Hα emission at a given disk radius than their B2 Ve counterparts because at this lower temperature the disk-to-star intensity ratio, the vertical scale height, and the thermal emission line broadening are all smaller.

The dotted line in Figure 1 shows how the Hα equivalent width is reduced when the outer boundary for the disk grid is moved inwards from $100R_s$ to $25R_s$ for the case of a B2 Ve

star with a disk inclination of 80° and a disk density exponent of $n = 3.0$. The outer disk region contains low brightness, optically thin gas, and although the emission contribution from any particular outer radius area element is small, the projected area of such elements increases with radius so that the selection of the outer boundary condition is important. We found that increasing the outer boundary from $100R_s$ to $200R_s$ for this parameter set increased the equivalent widths by only 10%, so we adopted the $100R_s$ boundary as our nominal choice. The selection of the boundary radius will mainly be important for Be stars in binary systems where the outer disk will be truncated by the gravitational influence of the companion.

Finally, the dot-dashed line in Figure 1 shows another sequence for the same B2 Ve, $i = 80°$, and $100R_s$ boundary case, but calculated this time with a larger disk density exponent of $n = 3.5$ (i.e., a steeper drop off in density). The overall shape of this curve is almost the same as the one for $n = 3.0$ (although the fiducial base density points have very different locations), and this suggests that the particular choice of density law is not important for the derived equivalent width – radius relationships. Investigations of the infrared flux excess in Be stars suggest that the exponent falls in the range $n = 2-4$ (Porter & Rivinius 2003). We caution that the results become more sensitive to the outer disk boundary for $n < 3$ where the emission from the optically thin, outer regions assumes more significance.

We have constructed such model sequences for subtypes B0, B2, B4, B6, and B8 Ve, for inclinations $i = 0°$, 50°, and 80°, and for outer boundary radii of $17R_s$, $25R_s$, $50R_s$, and $100R_s$. These numerical results, an interpolation program, and our code are available to interested readers at our Web site[1].

2. Comparison with Disk Radii from Interferometry

We can test the predictions of the model with the interferometric observations of nearby Be stars for which the projected disk shape and size in the sky are known. The long baseline interferometric observations in the narrow band surrounding Hα are fit with an elliptical Gaussian, and the reported diameter $\theta^d_{\rm mj}$ is the FWHM of the Gaussian fit to the major axis. We list in Table 1 the observed and adopted parameters for the Be stars with Hα interferometric observations from Quirrenbach et al. (1997) and Tycner et al. (2005, 2006). The columns of Table 1 list the star name, a contemporaneous measurement of W_λ and a code for the data source, adopted effective temperature (Zorec, Frémat, & Cidale 2005),

[1]http://www.chara.gsu.edu/~gies/Idlpro/BeDisk.tar

the stellar angular diameter determined from flux fitting methods (Underhill et al. 1979; Ochsenbein & Halbwachs 1982), the interferometric disk radius, ratio of the projected minor to major axis r, and a code for the data source, an estimate of the disk inclination, and finally the ratio R_d/R_s from interferometry and from W_λ (plus the adopted outer boundary for the calculation of the latter).

We determined the ratio R_d/R_s for each of the observations listed in Table 1 by interpolating in the model sequences for W_λ, $T_{\rm eff}$, i, and outer disk boundary. We estimated the disk inclination angle by equating the predicted value of the projected minor to major axis with the observed value,

$$r \approx \cos i + \frac{C_s}{V_{\rm K}} \sqrt{\frac{R_d}{R_s}} \sin i \qquad (6)$$

where the disk vertical dimension is evaluated at radial distance R_d, C_s is the speed of sound, and $V_{\rm K}$ is the Keplerian velocity at $R = R_s$ (see eq. [4] in Hummel & Vrancken 2000). The ratio $C_s/V_{\rm K}$ is ≈ 0.022 among main sequence B-stars for the temperatures, masses, and radii given by Harmanec (1988). We assumed an outer disk boundary of $100R_s$ for all but the known binary stars where we adopted the Roche radius of the primary star instead (Gies et al. 2006; Hubert et al. 1997).

The model disk radii predicted from W_λ are listed in Table 1 and compared to the interferometric radii in Figure 2. The predicted radii are generally in reasonable agreement with the observed radii, however, the model tends to overestimate the radii for a given equivalent width (or to underestimate the equivalent width for a given radius) for the weaker emission and cooler stars, η Tau and β CMi. Furthermore, the predicted radii of the stronger emission stars appear to be systematically lower than observed. We suspect that this latter problem is due to an underestimation of the true emission equivalent width in very active Be stars. If Be star disks contribute a fraction of the continuum flux in the V-band spectrum of $\epsilon = F^d_\lambda/F^s_\lambda$, then we need to renormalize the equivalent widths to $(1+\epsilon)W_\lambda$ in order to compare them with the model results where the equivalent width is referred to the stellar continuum alone. We lack direct information on the value of ϵ for the targets in Table 1, but we can approximately estimate the renormalization factor from the work of Dachs, Kiehling, & Engels (1988) who found that $(1+\epsilon) \approx (1 - 0.003W_\lambda)^{-1}$ based upon fits of the spectral energy distributions in a sample of Be stars (see their eq. [40]). The revised radii including this correction (*open squares* in Fig. 2) are in better agreement with the interferometric radii. Thus, the predictions of the models appear to be generally consistent with the available interferometric data.

The method outlined above offers a new way to estimate disk radius for distant Be stars that is based only upon the Hα equivalent width and estimates of spectral subtype, inclination, and outer disk boundary. It should prove to be a useful addition to the traditional

method from Huang (1972) that is based upon measurements of the separation between double peaks of the Hα profile and upon an assumed mass. We caution readers that the derived radii for individual targets are probably only accurate to within $\pm$30% at the moment (percentage standard deviation of the residuals for the dilution corrected radii in Fig. 2) and that higher precision will require detailed modeling of the spectral energy distribution and emission lines. Such models will probably need a more detailed physical description of the disk (Carciofi & Bjorkman 2006) with attention paid to possible asymmetries in the disk gas (Porter & Rivinius 2003). The effort involved is certainly merited in studies of selected Be stars, but the simpler approach presented here may be valuable in surveys of Be stars where observations are limited to low resolution spectroscopic measurements of the Hα equivalent width (or a photometric counterpart; McSwain & Gies 2005). The method will also be useful for planning future interferometric observations.

We are grateful to Dr. Christopher Tycner and an anonymous referee for their insight and comments that greatly aided our investigation. This work was supported by the National Science Foundation under Grant No. AST-0205297 and AST-0506573. Institutional support has been provided from the GSU College of Arts and Sciences and from the Research Program Enhancement fund of the Board of Regents of the University System of Georgia, administered through the GSU Office of the Vice President for Research.

REFERENCES

Apparao, K. M. V., Tarafdar, S. P., Verma, R. P., Iyengar, K. V. K., & Ghosh, K. K. 1993, J. Astrophys. Astr., 14, 135

Carciofi, A. C., & Bjorkman, J. E. 2006, ApJ, 639, 1081

Chesneau, O., et al. 2005, A&A, 435, 275

Dachs, J., Kiehling, R., & Engels, D. 1988, A&A, 194, 167

Gies, D. R., et al. 2006, ApJ, submitted

Harmanec, P. 1988, Bull. Astr. Inst. Cz., 39, 329

Horne, K. 1995, A&A, 297, 273

Horne, K., & Marsh, T. R. 1986, MNRAS, 218, 761

Huang, S.-S. 1972, ApJ, 171, 549

Hubert, A. M., et al. 1997, A&A, 324, 929

Hummel, W., & Vrancken, M. 1995, A&A, 302, 751

Hummel, W., & Vrancken, M. 2000, A&A, 359, 1075

Martins, L. P., González Delgado, R. M., Leitherer, C., Cerviño, M., & Hauschildt, P. 2005, MNRAS, 358, 49

McSwain, M. V., & Gies, D. R. 2005, ApJ, 622, 1052

Ochsenbein, F., & Halbwachs, J. L. 1982, A&AS, 47, 523

Porter, J. M., & Rivinius, Th. 2003, PASP, 115, 1153

Quirrenbach, A., et al. 1997, ApJ, 479, 477

Stee, Ph., de Araujo, F. X., Vakili, F., Mourard, D., Arnold, L., Bonneau, D., Morand, F., & Tallon-Bosc, I. 1995, A&A, 300, 219

Tycner, C., et al. 2005, ApJ, 624, 359

Tycner, C., et al. 2006, AJ, 131, 2710

Underhill, A. B., Divan, L., Prevot-Burnichon, M.-L., & Doazan, V. 1979, MNRAS, 189, 601

Zorec, J., Frémat, Y., & Cidale, L. 2005, A&A, 441, 235

Table 1. Be Stars with Interferometric Hα Measurements

Star Name	W_λ (Å)	Ref. Col. 2	$T_{\rm eff}$ (kK)	$\theta^\star$ (mas)	$\theta^d_{\rm mj}$ (mas)	r	Ref. Col. 6, 7	i (deg)	R_d/R_s (interferometry)	R_d/R_s (Hα)	R_d/R_s (boundary)
γ Cas	−29.1	1	30.2	0.45	3.47	0.70	2	49	7.7 ± 1.2	6.3 ± 0.9	27
γ Cas	−22.5	3	30.2	0.45	3.67	0.79	3	42	8.2 ± 1.2	5.3 ± 0.7	27
γ Cas	−31.2	4	30.2	0.45	3.59	0.58	5	58	8.0 ± 1.2	6.9 ± 1.1	27
ϕ Per	−35.0	1	28.8	0.26	2.67	0.46	2	67	10.1 ± 0.8	8.3 ± 1.4	22
ϕ Per	−42.6	4	28.8	0.26	2.89	0.27	5	79	10.9 ± 0.4	10.2 ± 1.9	22
ψ Per	−33.7	1	16.8	0.35	3.26	0.47	2	66	9.3 ± 0.7	9.2 ± 1.5	100
η Tau	−6.9	6	12.4	0.72	2.65	0.95	2	21	3.7 ± 0.2	5.2 ± 0.5	100
η Tau	−4.3	3	12.4	0.72	2.08	0.75	3	44	2.9 ± 0.3	5.4 ± 0.7	100
48 Per	−22.3	1	16.7	0.39	2.77	0.89	2	31	7.2 ± 1.5	7.4 ± 1.1	18
ζ Tau	−19.4	6	20.1	0.43	4.53	0.28	2	78	10.5 ± 1.2	8.6 ± 1.5	24
ζ Tau	−20.6	3	20.1	0.43	3.14	0.31	3	75	7.3 ± 0.5	8.7 ± 1.5	24
β CMi	−3.3	3	12.1	0.73	2.13	0.69	3	49	2.9 ± 0.7	5.5 ± 0.7	100

References. — 1. Hummel & Vrancken (1995); 2. Quirrenbach et al. (1997); 3. Tycner et al. (2005); 4. Gies et al. (2006); 5. Tycner et al. (2006); 6. Apparao et al. (1993).

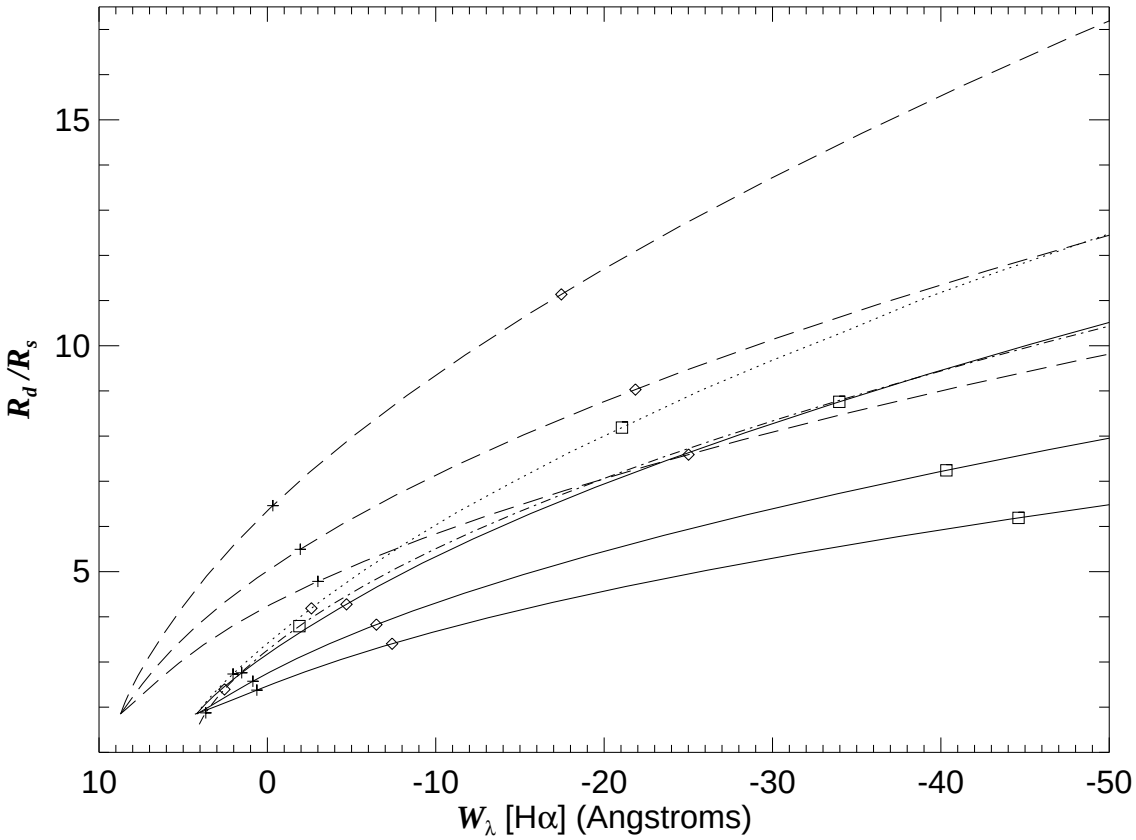

Fig. 1.— Plots of the predicted Hα equivalent width and disk half-maximum radius for several model sequences. The solid lines show the relationships for models with a B2 Ve central star, an outer boundary of $100R_s$, and inclinations of 0° (*bottom*), 50° (*middle*), and 80° (*top*). The three dashed lines show the results from models with the same inclinations but with a B8 Ve star. The dotted line shows how the relation changes for a model with a B2 Ve star and disk inclination of 80° when the outer boundary is reduced to $25R_s$. The dot-dashed line shows that the relation is almost identical for a model with a B2 Ve star, $i = 80°$, and $100R_s$ boundary when the disk density exponent is changed from $n = 3.0$ to 3.5. Disk base density values of $\rho_0 = 1 \times 10^{-12}$, 2×10^{-12}, and 5×10^{-12} g cm^{-3} are indicated along sequences by a plus sign, diamond, and square, respectively.

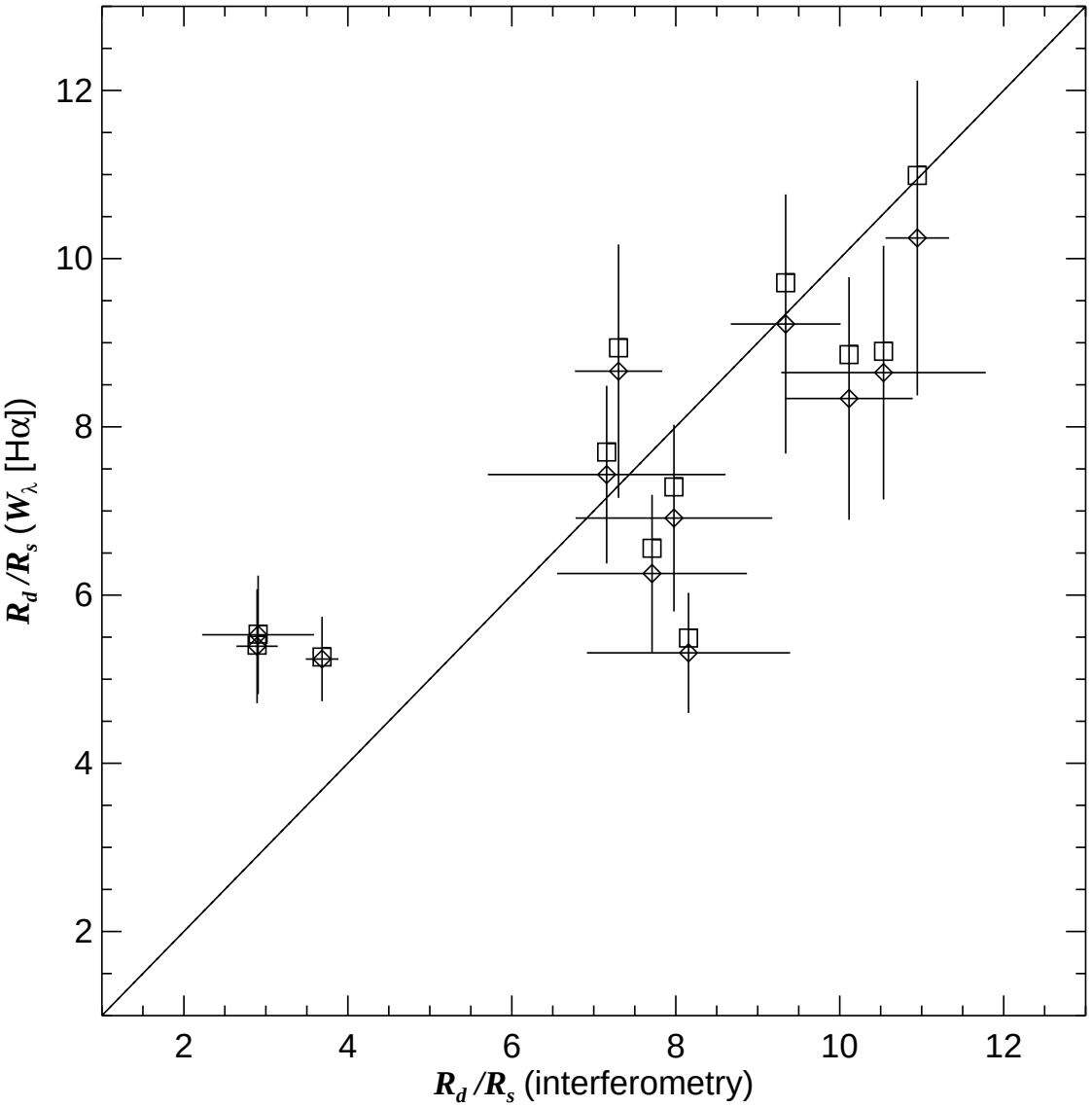

Fig. 2.— A comparison of the Hα disk radii obtained directly from interferometry with those predicted by the models using the Hα equivalent width (*diamonds* centered on the errors bars). The solid line shows the expected one-to-one correspondence. The open squares show how the predicted radii increase if the equivalent widths are renormalized to account for dilution by the disk continuum V-band flux (Dachs et al. 1988).